

# Vanadium and Melanoma

Subjects: Chemistry, Medicinal | Oncology

Contributor: Manuel Aureliano

Melanoma is the most aggressive type of skin cancer, the incidence of which has been increasing annually worldwide.

Keywords: vanadium ; vanadium complexes ; vanadium nanoparticles

---

## 1. Introduction

The past decades have marked important advances in the traditional view of many roles that metals and their compounds play in biological systems. In fact, metals, inorganic compounds and/or metals-organic frameworks show a diversity of properties that allowed them to present several and distinct biological, environmental and health applications <sup>[1][2][3][4][5][6][7][8][9][10][11][12][13][14][15][16][17][18][19]</sup>. Recent insights into metals applications includes for instance, zinc nanoparticles as feed additives showing more efficiency than zinc salts, increasing growth not only in fish <sup>[1]</sup> but also in plants <sup>[2]</sup>, besides preventing metal contaminants accumulation <sup>[2]</sup> and normalizing antioxidant biomarkers <sup>[1][2]</sup>. Very recently, zinc salts have been referred with a potential use in medicine such for the prevention and treatment of SARS-CoV-2 infection <sup>[3][4]</sup>. Polyoxotungstates (POTs), such as decatungstate ( $W_{10}O_{32}^{4-}$ ), have shown, by photocatalytic activity, to decompose antibiotics namely sulfasalazine and sulfapyridine with different specificities and rates <sup>[5]</sup>. Besides green biotechnology applications, it was suggested that some POTs hamper melanoma cancer cells growth through inhibition of aquaporin-3 activity <sup>[6]</sup>, whereas others POTs as well as gold compounds showed specific inhibitory activities for P-type ATPases <sup>[7][8]</sup>.

Removal of metal contaminants, such as for example cadmium, lead, arsenic and uranium from the environmental is still a problem to overcome in the 21st century. Recent studies highlighted the importance of uranyl speciation and the choice of specific chelating ligands for uranium removal and recovery from wastewater using electrocoagulation, being alizarin and iron electrode the most efficient combination <sup>[9]</sup>. On the other hand, metals contaminants such as cadmium are known to induce changes in biochemical parameters in brain causing neurological dysfunction that were proposed to be prevent by tomato and/or garlic extracts, in a rat model <sup>[10]</sup>. In humans, cadmium levels in urine were also found to be associated with an increase of LDL (low density lipoprotein)-cholesterol and a decrease of HDL (high density lipoprotein)-cholesterol, leading to an increased cardiovascular risk <sup>[11]</sup>.

Lithium, the well-known benefic metal and used in treatment of bipolar disease, has been recently described to partially prevent the increase of  $Na^+/K^+$ -ATPase activity induced by sleep privation, as observed in rats <sup>[12]</sup>. In humans, lithium showed to be a  $Na^+/K^+$ -ATPase regulator once it was verified that impede the decreased of the  $Na^+/K^+$ -ATPase activity observed in chorea-acanthocytosis patients <sup>[13]</sup>. Essential elements such as cobalt could be a good choice in hip prosthesis <sup>[14]</sup>. However, it was described that cobalt is accumulated and affects differently astrocytes and neurons, inducing cytotoxicity in brain cells <sup>[14]</sup>, whereas functionalized cobalt nanoflakes were described with anticancer activities <sup>[15]</sup>. Finally, a large number of different vanadium salts and complexes have been investigated and reported to have insulin enhancing, as well as anticancer properties <sup>[16][17]</sup>. Regarding vanadium and cancer, the number of articles found are higher for lung (n = 80), breast (n = 73) and liver (n = 70) cancer, medium for colon (n = 32), leukemia (n = 26) and bone (n = 21), whereas lower numbers of studies were found for brain (n = 10) and skin (n = 8), after a research in the Web of Science.

Although vanadium studies in skin cancer have being scarce, melanoma is the most aggressive type of skin cancer, and its incidence has been increasing annually worldwide at a faster rate compared to any other type of malignant tumor <sup>[20][21]</sup>. Usually, this pathology is diagnosed early and treated by surgery. On the other hand, its ability to metastasize makes this pathology dangerous <sup>[21]</sup>, which along with patients' relapse driven by the acquisition of therapy resistance <sup>[22]</sup>, makes the search for novel therapeutic targets and options for melanoma treatment a priority <sup>[23]</sup>.

This disease develops from melanocytes, cells found predominantly in the basal layer of the epidermis <sup>[20][24][25]</sup>. Melanocytes derive embryologically from pluripotent neural crest stem cells, which have high migratory potential <sup>[25][26]</sup>. This migratory embryonic origin of the melanocytes explains why melanoma is a type of cancer with a high capacity for

metastasis [25]. The homeostasis of these melanocytes is controlled by epidermal keratinocytes. These last cells produce a hormone called MSH (melanocyte stimulating hormone), which allows the binding between MC1R (melanocortin 1 receptor) and melanocytes, controlling melanocytes proliferation and preventing the appearance of changes in DNA, through the production of melanin [20]. When skin cells are exposed to excessive ultraviolet (UV) radiation, the formation of malignant melanocytes can be induced through two different mechanisms: direct transformation of normal melanocytes into cancerous melanocytes and the transformation of melanocytes into benign nevi, which subsequently become malignant (Figure 1). Direct targeting of melanocytes normally occurs when mutations in proto-oncogenes and tumor suppressor genes emergence (TP53, NF1, PTEN, etc.). When melanocytes are turned into benign nevi, these can stay that way for decades. However, UV rays can cause the appearance of genetic mutations in the TERT genes (reverse transcriptase of telomerase II) and CDKN2A (cyclin 2A-dependent kinase inhibitor) for example, which lead to malignant transformation of the nevi (Figure 1) [20].

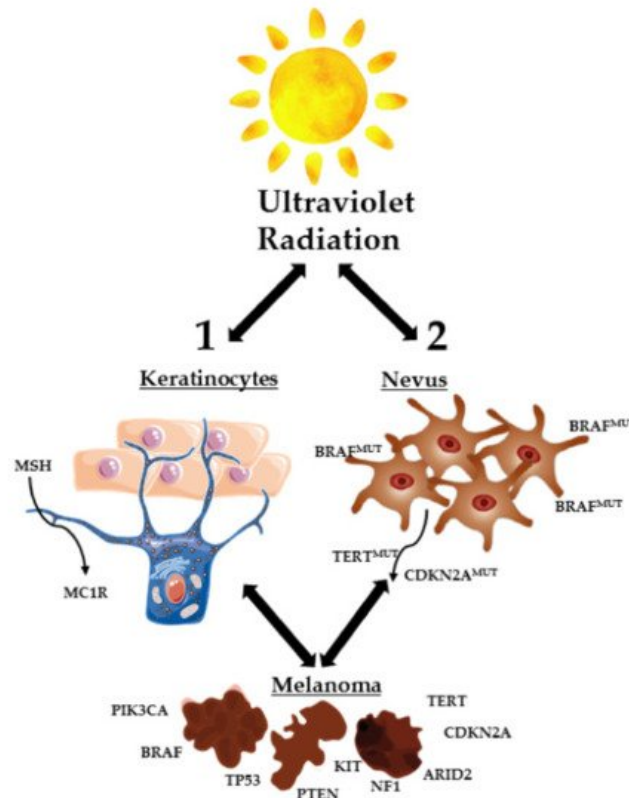


**Figure 1.** Skin cells exposed to excessive UV radiation. Formation of malignant melanocytes by direct transformation of normal melanocytes and/or transformation of melanocytes into benign nevi, which become malignant (adapted from [20]). ARID2, AT-rich interaction domain 2; BRAF, B-Raf proto-oncogene; CDKN2A, cyclin-dependent kinase inhibitor 2A; KIT, KIT proto-oncogene receptor tyrosine kinase; MC1R, melanocortin 1 receptor; MSH, melanocyte stimulating hormone; NF1, neurofibromin 1; PIK3CA, phosphatidylinositol-4,5-bisphosphate 3-kinase catalytic subunit alpha; PTEN, phosphatase and tensin homolog; TERT, telomerase reverse transcriptase; TP53, tumor protein p53.

## 2. Methodology

In this systematic review, the following databases were chosen: Clinical Trials, Cochrane Library, Pubmed/Medline, Scielo and Web of Science. Search terms used were: "Melanoma AND vanadium" and "Melanoma AND vanadate". The literature search was carried out between the 10 March 2021 and the 31 March 2021.

Inclusion and exclusion criteria were defined to select the articles with more relevance to this study (Figure 2, steps 5 and 6, respectively).

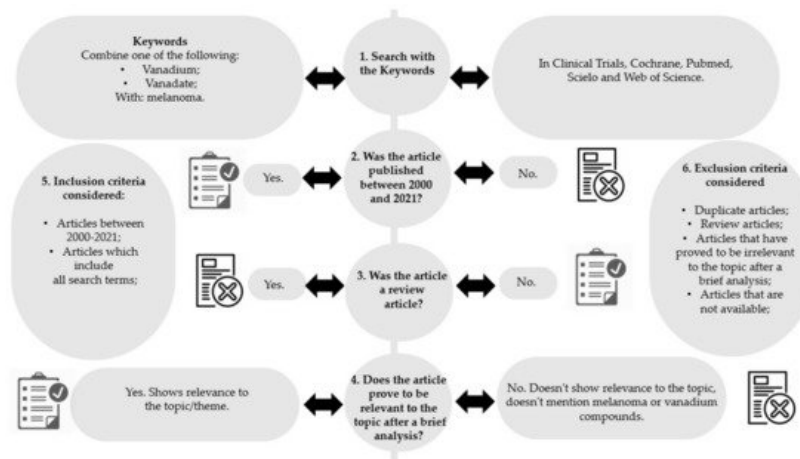


**Figure 2.** Methodology diagram of the articles' selection process.

After the initial research (Figure 2, step 1), articles which were relevant to the topic were selected by at least two independent researchers, by applying the following steps:


- Removal of articles not published between 2000 and 2021 (Figure 2, step 2);
- Removal of review articles (Figure 2, step 3);
- Evaluation of titles/abstracts and obtaining all articles potentially relevant;
- Confirmation of the relevance or irrelevance of the articles obtained, checking for factors that would imply inclusion/exclusion, through the reading of the full articles (Figure 2, step 4);
- Organization of selected studies in a reference management program.

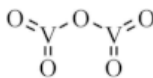
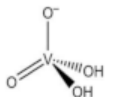
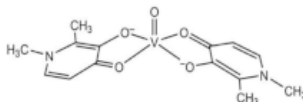
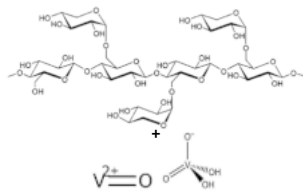
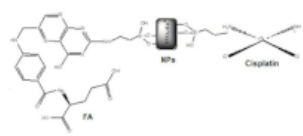
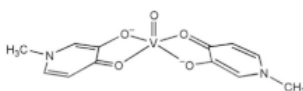
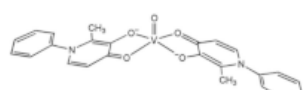
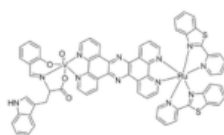
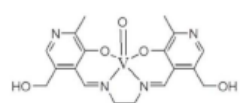
After selecting the articles with relevance to the topic, the data were grouped and treated. Subsequently, the results of the various investigations were studied, and the methods, doses and treatment durations, types of samples and models used, were analyzed. The summary of the methodology used is outlined in Figure 2. From the twenty-one studies found, twelve were eliminated, of which: nine articles for not being dated between 2000 and 2021; two articles because they were a review; and one article for being irrelevant to the topic. Finally, nine articles were considered for this review.

### 3. Types of Vanadium Based-Compounds Used in Studies against Melanoma

Among the eleven vanadium, vanadium complexes and/or materials found in the nine articles selected, eight are vanadium (IV), and/or vanadium (V) compounds, two represents vanadium nanoparticles (NPs) (compounds 3 and 7) and one is an emergent material from the family of early transition metal carbides/nitrides referred to as MXenes (compound 2) (Table 1). Regarding the eight vanadium(IV/V) solutions, seven are complexes of oxidovanadium (IV) and/or salts of oxidovanadium (compounds 1, 5, 6, 8, 9, 10 and 11) and one is the monomeric vanadate species itself (compound 4). The structure of these vanadium compounds and/or vanadium materials [27][28][29][30][31][32][33][34][35] are represented in Table 1. It should be noted that compound 6 can be formed with both vanadium oxidation states IV (oxidovanadium(IV)) and V (vanadate) being compounds 4 and 5 described in two articles [30][31], while compounds 5, 8 and 9 were referred in the same article [31] (Table 1).

**Table 1.** Representation of the structures of vanadium compounds and/or vanadium materials included in the entry.

Vanadium Compound/Material	Structure	Year
VOSO <sub>4</sub>		
Vanadyl sulfate (Abbreviated VO)	(VO <sup>2+</sup> ) V <sup>2+</sup> =O	2021
1		
V <sub>2</sub> CT <sub>z</sub> -ox <sub>24</sub> / V <sub>2</sub> CT <sub>z</sub> -ox <sub>48</sub> (V2CTz)		
Vanadium carbides (MXenes)	 s-V <sub>2</sub> CT <sub>z</sub>	2020
2		

Vanadium Compound/Material	Structure	Year
$V_2O_5$ Vanadium pentoxide (VP) 3		2020
$H_2VO_4^-$ monomeric vanadate (VN) 4		2019, 2017
$V^{IV}O(dhp)_2$ (VS2) dhp: 1,2-dimethyl-3-hydroxy-4(1H)-pyridinonate 5		2019, 2017
Xyloglucan oxovanadium (IV/IV) (XGCVO) 6		2018
$Y^{III}V^VO_4: Eu^{III}$ (YVEu NPs) Europium(III)-doped yttrium vanadate nanoparticles 7		2018
$[V^{IV}O(mpp)_2]$ (VS3) mpp: 1-methyl-3-hydroxy-4(1H) pyridinonate 8		2017
$[V^{IV}O(ppp)_2]$ (VS4) ppp: 1-phenyl-2-methyl-3-hydroxy-4(1H)-pyridinonate 9		2017
$[Ru-(pbt)_2(tpphz)VO(sal-L-try)]Cl_2$ (RuVO) pbt = 2-(2'-pyridyl)benzothiazole tpphz = tetrapyrrodo [3,2-a:2',3'-c:3'',2''-h:2''',3'''-j]phenazine sal-L-try = N-salicylidene-L-tryptophanate 10		2013
N,N'-ethylenebis (pyridoxylideneiminat) 		2013

## 4. Vanadium Species, Complexes and/or Materials Effects in Melanoma Cells

### 4.1. Cell Viability Effects

B16F10 cells (murine skin melanoma) were treated with several concentrations of vanadyl sulfate ( $VOSO_4$ ) (compound 1), treated with or without recombinant Newcastle disease virus (NDV). NDV, is an oncolytic agent that has been study in pre-clinical cancer models and human clinical trials [36]. After 48 h, the cellular metabolic ability was measured using the resazurin assay. Vanadyl plus NDV reduced the metabolic activity of B16F10 cells, showing that cell viability decreased between 45% and 90%, 90% at the highest concentration used of  $VOSO_4$  (200  $\mu$ M). The combination between vanadyl

(oxidovanadium(IV)) and the oncolytic agent NDV showed further decrease in cell viability than either  $\text{VOSO}_4$  or NDV alone, being dose-dependent. While using  $\text{VOSO}_4$  alone reduced over 50% of metabolic activity only from 100  $\mu\text{M}$  and above, the combination with NDV showed a similar inhibitory effect at the lowest dose of  $\text{VOSO}_4$  tested (0.78  $\mu\text{M}$ ) [27].

The effects of  $\text{V}_2\text{CTz-ox}_{24}/\text{V}_2\text{CTz-ox}_{48}$  (compound **2**) were studied in A375 cells (human malignant melanoma) and in HaCaT cells (immortalized keratinocytes). Cells were treated with several concentrations of the two MXenes and an MTT (3-(4,5-dimethylthiazol-2-yl)-2,5-diphenyltetrazolium bromide) assay was done to measure the metabolic activity of the cells, as a measure of cellular viability. Comparing both MXenes, the results showed that  $\text{V}_2\text{CTz-ox}_{48}$  provided a higher decrease in cell viability: in A375 cells, cells viability decreased between 28–65%; in HaCaT cells, cells viability decreased between 25% and 60%.  $\text{V}_2\text{CTz-ox}_{24}$  showed a decrease between 15% and 55% in A375 cells and between 2% and 30% in HaCaT cells. The highest decrease in cell viability was detected at the highest concentrations used (200  $\mu\text{g/mL}$ ), in both cell lines. While a decrease of 50% of cellular viability was observed with 25–50  $\mu\text{g/mL}$  of  $\text{V}_2\text{CTz-ox}_{24}$  only in A375 melanoma cells, a comparable inhibitory effect was achieved with 1–5  $\mu\text{g/mL}$  of  $\text{V}_2\text{CTz-ox}_{48}$ , in both cell lines [28].

B16F10 cells were treated with several concentrations of vanadium pentoxide ( $\text{V}_2\text{O}_5$ ) (compound **3**) during 24 h. The MTT assay showed that the viability of the cells, treated with increasing doses of  $\text{V}_2\text{O}_5$ , decreased up to 70% with the highest concentration used (50  $\mu\text{g/mL}$ ), showing dose-dependent inhibition levels between 15% and 70%. A decrease of 50% of cellular viability was observed upon treatment with 10  $\mu\text{g/mL}$  in melanoma cells [29].

Cytotoxic activity for compounds **4**, **5**, **8** and **9** (VN, VS2, VS3, and VS4, respectively) was evaluated by MTT assay in A375 and CN-mel (human noncutaneous metastatic melanoma [32]) cells. Both cell lines were treated for 72 h at three different concentrations (1, 10 and 100  $\mu\text{M}$ ) of each vanadium compound [30][31]. At the lowest concentration, cells did not show accentuated signs of decreased cell viability. On the other hand, at 10 and 100  $\mu\text{M}$ , A375 cells underwent a marked decrease in cell viability, presenting viability values never greater than 2% for all compounds, regardless of the concentration tested. CN-mel showed a less accentuated decrease, having viability values between 52% and 59% at 10  $\mu\text{M}$  but even so, at the highest concentration (100  $\mu\text{M}$ ), there was a more pronounced decrease viability, with viability values between 1.5% and 13%. In these conditions,  $\text{IC}_{50}$  values between 2.4 and 4.7  $\mu\text{M}$  were found for A375 cells and between 6.5 and 14  $\mu\text{M}$  for CN-mel cancer cells. The relative order of potency for human noncutaneous metastatic melanoma was found to be compound **4** > **8** > **5** > **9** whereas for human malignant melanoma, the potency was different namely compound **8** > **5** > **9** > **4**.

B16F10 cells were treated with several concentrations of compound **6**, XGC:VO, which was cytotoxic in a concentration-dependent fashion. After 24 h of incubation, XGC:VO treatment decreased cells viability by 23% and 50% at 2.5  $\mu\text{g/mL}$  and 300  $\mu\text{g/mL}$ , respectively, though similar to what was observed with the polysaccharide XGC alone [32].

When treated with compound **11**,  $\text{Pyr}_2\text{enVO}$ , in the only concentration used (50  $\mu\text{M}$ ) and incubated for 72 h, the results showed 93% of cell death in A375 cells. Under these conditions,  $\text{IC}_{50}$  values ( $\mu\text{M}$ ) of 61.5 (24 h), 13.0 (48 h) and 6.0 (72 h) were found. Similarly, when treated with  $\text{Pyr}_2\text{en}$  solo (50  $\mu\text{M}$ ), cell mortality in A375 cells was around 18% [35].

## 4.2. Cell Morphology and Apoptosis Effects

To find out if apoptosis or necrosis occurs when A375 melanoma cells are incubated with compound **2**  $\text{V}_2\text{CTz-ox}_{24}/\text{V}_2\text{CTz-ox}_{48}$  for 24 h, a cytometric analysis using Annexin V-FITC and propidium iodide (PI) was performed. When performed in HaCaT cells, the results showed that the population of apoptotic cells was negligible, showing that the MXenes are biocompatible with keratinocytes (over 70% survivability). A375 cells exposed to the highest concentrations of s- $\text{V}_2\text{CTz-ox}_{48}$  showed the highest percentage of necrotic cells [28].

B16F10 cells were incubated with compound **3** ( $\text{V}_2\text{O}_5$ ) and with SU-5416 (semaxanib) for 18 h [29]. SU-5416 was used as a positive control, since this substance is an inhibitor of angiogenesis and leads to suppression of tumors through the induction of apoptosis [35][36]. Flow cytometry assay showed that cells treated with  $\text{V}_2\text{O}_5$  or with SU-5416 showed an increase in the apoptotic region in the single tested concentration (10  $\mu\text{g/mL}$ ), in relation to untreated cells. A TUNEL assay was also performed in the same conditions and the results exhibited TUNEL positivity with  $\text{V}_2\text{O}_5$  (10  $\mu\text{g/mL}$ ) and SU-5416 (20 nM) for 18 h, indicating DNA damage.

Apoptosis evaluation tests were performed on cells treated with compounds **4** and **5** (VN and VS2, respectively) in two different articles [30][31], having counted the live, apoptotic and necrotic cells. In Pisano, et al. [30] untreated and treated cells were also treated with NAC (N-acetylcysteine), a ROS inhibitory compound [39], as control. The Annexin V apoptosis assays suggested that treatments with the longer duration (48 h) and higher doses cause a larger apoptotic effect in A375 cells. VN increased apoptotic population up to 48%, while VS2 increased apoptotic population up to 52%, at the highest concentration used (20  $\mu\text{g/mL}$ ) in 48 h assays. In Rozzo, et al. [31], the Annexin V apoptosis assays suggested that

treatments with the longer duration (72 h) and higher doses cause larger apoptotic effects in A375 cells, as well. VN increased apoptotic population up to 70%, while VS2 increased apoptotic population up to 67%, at the highest concentration used (20 µg/mL) in 72 h assays.

Apoptotic analysis using flow cytometry was carried out to study the apoptotic effects of compound **6** (XGC:VO) and XGC alone, in B16F10 cells [32]. Cells were studied after 24 h treatments. The number of apoptotic cells increased 50% after treatment with XGC:VO, at the highest concentration used (200 µg/mL). In additional concentrations (5 and 25 µg/mL) and in cells treated with XGC (in all concentrations used), the appearance of apoptotic cells was considered by the authors to be mild.

Finally, cell morphology changes were described for compound **10** [34]. This, in the tests with the compound **10**, Ru-(pbt)<sub>2</sub>(tpphz)VO(salt-L-trypp), malignant cells of human amelanotic melanoma were used. The studies were carried out at concentrations of 5 and 20 µM, differing in the absence/presence of light. Both conditions were treated in the same way. Briefly, after 24 h of treatment, cells were incubated for 30 min in light or in the dark, and after 3 h the photos were taken using the microscope. The results indicated that death occurred in treated cells in the presence of light at the highest concentration of compound **10** (20 µM), although there are also some effects at the lowest concentration (5 µM). [Table 2](#) includes the effects referred above for the cellular viability, morphology and apoptosis effects of the vanadium compounds, as well as the effects described in the following sections namely: cell cycle effects, ROS production, mitochondrial effects, proteins expression studies and additionally in vivo anticancer activities such as tumor regression and survival rates.

**Table 2.** Vanadium compounds and materials effects in human melanoma cells lines, namely A375 (human malignant melanoma), CN-mel (human metastatic melanoma), amelanotic melanoma and B16F10 (Mus musculus skin melanoma) namely in: Cell viability, cell morphology and apoptosis effects, cell cycle effects, ROS production, mitochondrial effects and protein expressions. Mice in vivo anticancer studies are also included.

Compound	Cell Viability	Cell Morphology and Apoptosis Effects	Cell Cycle Effects	ROS Production	Mitochondrial Effects	Protein Expressions Studies	In Vivo Anticancer Activity
VO 1	B16F10 cells						Mice Tumor regression upon VOSO <sub>4</sub> (40 mg/kg), 96 h
	200 µM produces 90% inhibition, after 48 h						
V <sub>2</sub> CTz 2	A375 cells						
	50% inhibition for 1–5 µg/mL V <sub>2</sub> CTz-ox <sub>48</sub> and for 25–50 µg/mL V <sub>2</sub> CTz-ox <sub>24</sub>	A375 cells The population of apoptotic cells was negligible, for 24 h	A375 cells Cellular cycle arrest in the G0/G1 phase, triggering apoptosis	A375 cells V2CTz-ox24 increased ROS to 225%, (100 µg/mL) V2CTz-ox48 increased ROS to 140% (100 µg/mL)	A375 cells s-V2CTz-ox48, slight increase mitochondrial membrane potential (ΔΨm)		
VP 3	B16F10 cells						Mice The survival rate increased up to 47 days, (10 mg/kg) No changes: body weight; in feed intake. No toxicity in vital organs
	50% inhibition for 10 µg/mL	B16F10 cells Increase of apoptosis (10 µg/mL), for 18 h DNA damage (10 µg/mL), for 18 h		B16F10 cells Anion superoxide formation (10 µg/mL)		B16F10 cells Upregulation of p53 downregulation of anti-apoptotic survivin (10, 20 µg/mL)	

Compound	Cell Viability	Cell Morphology and Apoptosis Effects	Cell Cycle Effects	ROS Production	Mitochondrial Effects	Protein Expressions Studies	In Vivo Anticancer Activity
VN 4	A375 cells IC <sub>50</sub> = 4.7 μM, 72 h	A375 cells Pisano, et al. Increased apoptotic population to 48%, (20 μg/mL), 48 h. Rozzo, et al. Increased apoptotic population to 70%, (20 μg/mL), 72 h	A375 cells Cells did not go through the G2/M phase, dying through apoptosis	A375 cells ROS increased to 80% (20 μg/mL), 48 h.		A375 cells ph-ERK, ph-Rb and ph-Cdc25c levels decreased to 20% (20 μM), 24 h, p21Cip1 rised up to 10-14 times (20 μM)	
	CN-mel IC <sub>50</sub> = 6.5 μM, 72 h						
VS2 5	A375 cells IC <sub>50</sub> = 2.6 μM, 72 h	A375 cells Pisano, et al. Increased apoptotic population up to 52%, at the highest concentration used (20 μg/mL) in 48 h assays. Rozzo, et al. Increased apoptotic population up to 67%, at the highest concentration used (20 μg/mL) in 72 h assays	A375 cells Cell cycle arrested in G0/G1 phase, showing not to be able to enter the S phase.	A375 cells ROS levels increasing up to 80% as well, at the highest duration (48 h) and dose (20μg/mL).		Pisano, et al. A375 cells ph-ERK, ph-Rb and ph-Cdc25c levels decreased to 20% (20 μM), p21Cip1 levels increased up to 18 times (20 μM) Rozzo, et al. Increasing of the cleaved PARP band (85 kD)	
	CN-mel IC <sub>50</sub> = 12.4 μM, 72 h						
XGCVO 6	B16F10 cells  50% inhibition at 300 μg/mL	B16F10 cells 50% increase of apoptosis (200 μg/mL)	B16F10 cells Cell cycle has not changed		B16F10 cells Mitochondrial respiration decreased to 43% (5 μg/mL) 34% pyruvate decrease No effects lactate production		
YVEu NPs 7							Mice Tumor regression upon Y <sup>III</sup> V <sup>VO</sup> <sub>4</sub> :Eu <sup>III</sup> . CPTES:FA: CDDP (15 mg/kg), 5 days; CDDP toxicity reduced
VS3 8	A375 cells IC <sub>50</sub> = 2.4 μM, 72 h						
	CN-mel IC <sub>50</sub> = 10.4 μM, 72 h						
VS4 9	A375 cells IC <sub>50</sub> = 4.2 μM, 72 h						
	CN-mel IC <sub>50</sub> = 14.0 μM, 72 h						

Compound	Cell Viability	Cell Morphology and Apoptosis Effects	Cell Cycle Effects	ROS Production	Mitochondrial Effects	Protein Expressions Studies	In Vivo Anticancer Activity
RuVO 10		Amelanotic melanoma In the absence of light, changes in cell morphology (20 $\mu$ M). In the presence of light, apoptosis observed, 20 $\mu$ M.					Mice The survival rate was 100%. Tumor weight reduction. Proliferative activity reduction
Pyr <sub>2</sub> enVO 11	A375 cells IC <sub>50</sub> = 61.5 (24 h) IC <sub>50</sub> = 13.0 (48 h) IC <sub>50</sub> = 6.0 (72 h)		A375 cells Increase of G0/G1 cells to 60% (100 $\mu$ M), 72 h	A375 cells ROS increased to 23% (100 $\mu$ M), 24 h	A375 cells Percentage of cells with loss of $\Delta\Psi$ m increased up to 35% (100 $\mu$ M), 48 h, and 73%, after 72 h		

### 4.3. Cell Cycle Effects

To assess the effects on the cell cycle of cells treated with compound **2** (V<sub>2</sub>CTz-ox24 and V<sub>2</sub>CTz-ox48), a PI staining was performed. HaCaT cells suffered a small increase of G0/G1 phase in the maximum duration treatment (48 h), leading to an increased cell size. A375 suffered cellular cycle arrest in the G0/G1 phase, triggering apoptosis. A small increase in the number of melanoma cells in G2/M phase was observed [28].

Tests were carried out on A375 cells, with compounds **4** and **5** (VN and VS2, respectively), to evaluate the effects on cell cycle progression through PI cell staining [31]. Cells treated with two different concentrations of VN and VS2 (10 and 20  $\mu$ g/mL), for 24 h, 48 h and 72 h, were studied. Cells treated with compound **4** (VN) for 48 h and 72 h did not survive for such periods, so it was not possible to evaluate the cell cycle progression. When treated with compound **4**, VN, for 24 h, A375 cells did not go through the G2/M phase, dying through apoptosis. In cells treated with compound **5**, VS2, the cell cycle arrested in G0/G1 phase, showing not to be able to enter the S phase [31].

After A375 cells were treated with several concentrations of compound **11** Pyr<sub>2</sub>enV(IV), they were labeled with PI and subsequently analyzed by flow cytometry to measure the percentage of apoptotic nuclei sub-G0/G1. Cells treated with the highest concentration used (100  $\mu$ M) showed a percentage of Sub G0/G1 cells over 60%, in 72 h treatments. The results showed to be dose and duration dependents [35].

### 4.4. Effects on ROS Production

The level of intracellular reactive oxygen species (ROS) was measured using non-specific fluorescent dye (DCF-DA), when HaCaT and A375 cells were incubated with different concentrations of compound **2** (V<sub>2</sub>CTz-ox24 and V<sub>2</sub>CTz-ox48) for 48 h. V<sub>2</sub>CTz-ox24 increased ROS levels up to 225% in A375 cells (100  $\mu$ g/mL) and ~210% in HaCaT cells (50  $\mu$ g/mL). ROS levels caused by incubation with V<sub>2</sub>CTz-ox48 showed lower ROS levels in A375 cells compared to the other MXene, increased only up to 140% at the highest concentration (100  $\mu$ g/mL). In HaCaT cells, ROS levels increased up to 245%, at 50  $\mu$ g/mL with V<sub>2</sub>CTz-ox48, being the highest value obtained (Table 2) [28].

B16F10 cells were treated with DHE (dihydroethidium) reagent after compound **3** V<sub>2</sub>O<sub>5</sub> nanoparticles (10  $\mu$ g/mL) and SU-5416 (20 nM) exposure to determine the intracellular anion superoxide production. Cells treated with V<sub>2</sub>O<sub>5</sub> or SU-5416, displayed red fluorescence indicating the formation of intracellular ROS, suggesting that the formation of superoxide could be the plausible mechanism for the anticancer activity of vanadium pentoxide [29].

A375 cells were treated with compounds **4** and **5**, VN and VS2 and the percentage of ROS that appeared after treatments was measured through flow cytometry assay [30]. Percentages of ROS were checked in absence/presence of NAC (N-acetylcysteine). The increase of ROS with VN showed to be dependent on the treatment duration, showing no differences between the two doses used (10 and 20  $\mu$ g/mL). ROS formation increased up to ~78% at the highest duration (48 h) and dose (20  $\mu$ g/mL) used. VS2 showed to be dependent on the duration and dose of the treatment, showing ROS formation increasing up to ~78% as well, at the highest duration (48 h) and dose (20  $\mu$ g/mL) [30].



In the studies of compound **11** Pyr<sub>2</sub>enVO assay, A375 cells were also treated with Pyr<sub>2</sub>en alone and NAC was also used to inhibit the generation of ROS [35]. The results, obtained through flow cytometry, showed that the percentage of ROS formation did not exceed 23% (with or without NAC), reaching this value in cells treated for 24 h with the single tested concentration (100 µM) of Pyr<sub>2</sub>enVO. The increase of ROS was dependent of the duration of treatment. Cells treated with Pyr<sub>2</sub>en alone did not show ROS generation [35].

#### 4.5. Effects on Mitochondria Function

Mitochondrial activity after the exposure of A375 and HaCaT cells to compound **2** s-V<sub>2</sub>CTz-ox24 and s-V<sub>2</sub>CTz-ox48 at several concentrations was determined by monitoring the level of mitochondrial membrane potential ( $\Delta\Psi_m$ ) using the JC-10 dye [28]. HaCaT cells suffered a slight decrease in the  $\Delta\Psi_m$ , in the presence of both MXenes. On the other hand, A375 cells exposed to s-V<sub>2</sub>CTz-ox48 suffered a slight increase of the  $\Delta\Psi_m$ .

The effects on the respiration of B16F10 cells treated with compound **6** XGC:VO (5 and 25 µg/mL) for 24 h were studied by high-resolution respirometry in an Oxygraph-2k [32]. The results showed an inhibition of cellular respiration. Thus, in the basal state, cells respiration decreased up to 43% and 54% in treatments with 5 and 25 µg/mL, respectively. On the uncoupled state, XGC:VO inhibited the cells respiration up to 60% in treatments with 5 and 25 µg/mL. The effects of XGC:VO (5 and 25 µg/mL for 24 h) in the production of lactate and pyruvate by B16F10 cells were also studied. The treatment with the complex resulted in a decrease of about 34% and 22.5% in the production of pyruvate, for concentrations 5 and 25 µg/mL, respectively. Still, XGC:VO did not alter the production of lactate (Table 2).

Finally, measurement of mitochondrial membrane potential ( $\Delta\Psi_m$ ) was done by flow cytometry (FL-2 channel) in A375 cells treated with 100 µM of compound **11** Pyr<sub>2</sub>enVO or vehicle (Pyr<sub>2</sub>en) for 24, 48 and 72 h. The results showed that the percentage of cells with a potential loss was 34.65% after 48 h and rose to 73.24% after 72 h [35].

#### 4.6. Protein Expressions Effects

To begin dissecting cellular mechanisms of action, B16F10 cells treated with compound **3** V<sub>2</sub>O<sub>5</sub> NPs (10–20 µg/mL) were studied through Western blot, checking the differential apoptotic proteins expression. The results demonstrated upregulation of p53 and downregulation of anti-apoptotic protein survivin, corroborating with the apoptosis and cell cycle analysis [29].

In Pisano, et al. [30], A375 cells were treated with the compounds **4** and **5**, VN and VS2, at two different concentrations (10 and 20 µM), for several time intervals (3, 6, 16 and 24 h). To study the levels of expression and/or activation of some key proteins that regulate the initiation and progression of cell cycle, Western blot experiments were carried out using specific antibodies for several proteins. A375 cells, after treatments with VN and VS2, suffered a gradual decrease up to 20% in the levels of ERK phosphorylation (P-ERK). On the other hand, the levels of total ERK protein expression remained unchanged, after both treatments. Levels of P-Rb suffered a gradual decrease, reaching levels of 0% and 10%, respectively after 16 h of treatments with VN (20 µM) and after 24 h of treatments with VS2 (10 µM). The expression of the CDK inhibitor p21Cip1 increased during the first hours (3 and 6 h) of treatment with the two compounds. p21Cip1 increased up to 10-14 times in compound **4**, VN-treated cells, and up to 18 times in VS2 treated cells. When P-Cdc25c was studied, the results showed a 20% and 10% decrease in 10 and 20 µM VN/VS2 treated cells, respectively. After treatments with compound **5**, VS2 (10 and 20 µM), A375 cells were subjected to a Western blot in Rozzo, et al. [31]. The assay showed an increasing of the cleaved PARP band (85 kD) and decreasing of the whole PARP band (116 kD), dose-dependent, confirming apoptosis (Table 2).

#### 4.7. Anticancer Effects In Vivo

C57BL/6 mice were implanted with B16F10 tumor cells intradermally and when the tumors reached 5 mm in diameter, the treatments were initiated. The groups of animals were either injected intratumorally with phosphate-buffered saline (PBS), compound **1** VOSO<sub>4</sub> (20 mg/kg or 40 mg/kg), Newcastle disease virus (NDV) solo, or a combination of VOSO<sub>4</sub> plus NDV, every 48 h for a total of 3 treatments. The treatments ended when tumors reached 15 mm in a single direction. The results showed that there was a fast tumor regression in mice treated with VOSO<sub>4</sub> (40 mg/kg) plus NDV, after only 96 h. On the other hand, when mice were treated with a lower dose of VOSO<sub>4</sub> (20 mg/kg) plus NDV, 50% of the mice were cured of their disease [27]. After the animals were cured, the authors studied the hypothesis that treatment induced a tumor-specific memory. Mice were once again injected with B16F10 tumor cell, intravenously and subcutaneously, without any treatments there was no increase in survival rate when compared to controls, disproving the proposed hypothesis [27].

Still regarding compound 1, the effects on the tumor microenvironment (TME) and in tumor-draining lymph nodes (TdLNs) were studied. When tumors reached 8 mm in any one direction, the therapy was administered and after 36 h tumors were harvested from the mice. The therapy consisted in a single intratumoral treatment with PBS, vanadyl sulfate (40 mg/kg), NDV or in a combination of vanadyl sulfate plus NDV. Several leukocyte subsets were quantified by flow cytometry and the results showed that the relative number of IFN- $\gamma$  (producing NK cells) in the TME and in TdLNs increased in the combination treatment, indicating that this therapy potentiates the innate immune response [27].

It was also studied the cytotoxic potential of NK cells and the presence of M2 macrophages in tumors harvest from mice administered with a single intratumoral injection of PBS, vanadyl sulfate (40 mg/kg), NDV ( $5.0 \times 10^7$  PFU), or vanadyl sulfate 4 h prior to NDV, after 24 h. It was performed tumor-infiltrating lymphocyte (TIL) analysis using a specific antibody panel for this concrete study. The results showed that vanadyl sulfate plus NDV provoked the highest percentage of NK cells producing granzyme B, a cytotoxic serine protease found in the granules of NK cells. The results also showed that the number of M2 macrophages, identified through the presence of CD206, was reduced in treatments with vanadyl sulfate plus NDV. The therapy with vanadyl sulfate plus NDV enhanced the cytolytic potential of NK cells, while simultaneously decreased the immunosuppressive nature of the tumor microenvironment [27]. To investigate how this combination therapy alters the cytokine profile in the tumor microenvironment, tumor's cytokines were quantified in tumors harvested 36 h after treatments with PBS, vanadyl sulfate (40 mg/kg), NDV ( $5.0 \times 10^7$  PFU) or of vanadyl sulfate in combination with NDV, using a flow cytometry. There was an increase in the percentages of IFN- $\gamma$ , GM-CSF, MCP-1 (CCL2) and IL-6, while there was a decrease in percentages of IL-1 $\beta$ . Also, NDV or vanadyl sulfate plus NDV both increased the percentages of CXCL-10 and CCL5. The combination therapy showed changes in the cytokine profile in the TME.

To study the efficacy of compound 2  $V_2O_5$  in vivo, female C57BL/6J mice were injected subcutaneously in the lower right abdomen with B16F10 cells [29]. Later, a study was carried out to verify the animals' ability to survive. Thus, four groups of three mice were treated with different concentrations of vanadium pentoxide (0, 1, 5 and 10 mg/kg). Doses were administered intra-peritoneally when tumors reached 50–10 mm<sup>3</sup>, every 7 days. It was found that after treatments, the animals' survival rate increased, in comparison to untreated mice, at the highest dose used. It was also performed an assay to study the sub chronic toxicity of  $V_2O_5$ . Three groups of 5 mice were treated with 0, 10 mg/kg of  $V_2O_5$  NPs and 20 mg/kg of  $V_2O_5$  NPs, injected intra-peritoneally for 7 consecutive doses for a period of 28 days. The results showed that  $V_2O_5$  NPs did not bring changes in body weight or in feed intake. After sacrifice of the mice that underwent the study of sub chronic toxicity, several analyses to assess the effects caused by the administration of  $V_2O_5$ , namely a histopathological analysis, were performed. Globally, the mice did not show changes in the organs, and only some changes appeared, such as fatty degeneration in the liver tissues (when treated with a dose of 20 mg/kg) and mild peribiliary fibrosis (when treated with a dose of 10 mg/kg).

Finally, the antitumor efficiency of chemotherapy with cisplatin (CDDP) alone and incorporated into the compound 7  $Y^{III}VO_4:Eu^{III}$  NPs in vivo, was evaluated [33]. Male C57BL/6 mice were injected subcutaneously into the right dorsolateral region with viable B16F10 cells. When the tumor had reached approximately 100 mm<sup>3</sup> (18 days after cell implantation), five groups of five mice were treated with different compounds, such as 15 mg/kg of  $Y^{III}VO_4:Eu^{III}$ , 15 mg/kg of  $Y^{III}VO_4:Eu^{III}$ : CPTES (3-chloropropyltrimethoxysilane), 15 mg/kg of  $Y^{III}VO_4:Eu^{III}$ :CPTES:CDDP, 15 mg/kg of  $Y^{III}VO_4:Eu^{III}$ : CPTES:FA:CDDP and 5 mg/kg of CDDP, once a day and for 5 consecutive days. The survival rate of the mice studied was 70% in the CDDP group and 100% in all other groups. Furthermore, the group treated with CDDP solo, exhibited weight loss and liver weight decreased about 44%. It was observed that there was tumor weight reduction when treated with  $Y^{III}VO_4:Eu^{III}$ :CPTES:CDDP,  $Y^{III}VO_4:Eu^{III}$ : CPTES:FA:CDDP and CDDP, but not when treated with  $Y^{III}VO_4:Eu^{III}$  and  $Y^{III}VO_4:Eu^{III}$ : CPTES.

After the sacrifice of the mice, histopathological analysis showed a reduction in proliferative activity in mice treated with  $Y^{III}VO_4:Eu^{III}$ :CPTES:CDDP,  $Y^{III}VO_4:Eu^{III}$ : CPTES:FA:CDDP and CDDP, but not when treated with  $Y^{III}VO_4:Eu^{III}$  and  $Y^{III}VO_4:Eu^{III}$ :CPTES. It was also performed a micronucleus assay through Trypan blue exclusion, which assesses the frequency of micronuclei (genotoxic damage indicators) and this showed that there is a greater micronuclei formation in animals treated with  $Y^{III}VO_4:Eu^{III}$ :CPTES:CDDP only. Biochemical analysis suggested that treatment with CDDP causes nephrotoxicity [33]. The effects described above are briefly summarized in [Table 2](#).

---

## References

1. Mondal, A.H.; Behera, T.; Swain, P.; Das, R.; Sahoo, S.N.; Mishra, S.S.; Das, J.; Ghosh, K. Nano zinc vis-à-vis inorganic Zinc as feed additives: Effects on growth, activity of hepatic enzymes and non-specific immunity in rohu, Labeo rohita (Hamilton) fingerlings. *Aquac. Nutr.* 2020, 26, 1211–1222.

2. Yan, S.; Wu, F.; Zhou, S.; Yang, J.; Tang, X.; Ye, W. Zinc oxide nanoparticles alleviate the arsenic toxicity and decrease the accumulation of arsenic in rice (*Oryza Sativa* L.). *BMC Plant Biol.* 2021, 21, 150.
3. Carofiglio, M.; Barui, S.; Cauda, V.; Laurenti, M. Doped zinc oxide nanoparticles: Synthesis, characterization and potential use in nanomedicine. *Appl. Sci.* 2020, 10, 5194.
4. Arentz, S.; Hunter, J.; Yang, G.; Goldenberg, J.; Beardsley, J.; Myers, S.P.; Mertz, D.; Leeder, S. Zinc for the prevention and treatment of SARS-CoV-2 and other acute viral respiratory infections: A rapid review. *Adv. Integr. Med.* 2020, 7, 252–260.
5. Cheng, P.; Wang, Y.; Sarakha, M.; Mailhot, G. Enhancement of the photocatalytic activity of decatungstate, W<sub>10</sub>O<sub>32</sub>4–, for the oxidation of sulfasalazine/sulfapyridine in the presence of hydrogen peroxide. *J. Photochem. Photobiol. A Chem.* 2021, 404, 112890.
6. Pimpão, C.; da Silva, I.V.; Mósca, A.F.; Pinho, J.O.; Gaspar, M.M.; Gumerova, N.I.; Rompel, A.; Aureliano, M.; Soveral, G. The aquaporin-3-inhibiting potential of polyoxotungstates. *Int. J. Mol. Sci.* 2020, 21, 2467.
7. Gumerova, N.; Krivosudsky, L.; Fraqueza, G.; Breibeck, J.; Al-Sayed, E.; Tanuhadi, E.; Bijelic, A.; Fuentes, J.; Aureliano, M.; Rompel, A. The P-type ATPase inhibiting potential of polyoxotungstates. *Metallomics* 2018, 10, 287–295.
8. Fonseca, C.; Fraqueza, G.; Carabineiro, S.A.C.; Aureliano, M. The Ca<sup>2+</sup>-ATPase inhibition potential of gold (I,III) compounds. *Inorganics* 2020, 8, 49.
9. Li, P.; Chen, P.; Wang, G.; Wang, L.; Wang, X.; Li, Y.; Zhang, W.; Jiang, H.; Chen, H. Uranium elimination and recovery from wastewater with ligand chelation-enhanced electrocoagulation. *Chem. Eng. J.* 2020, 393, 124819.
10. Vijaya, P.; Kaur, H.; Garg, N.; Sharma, S. Protective and therapeutic effects of garlic and tomato on cadmium-induced neuropathology in mice. *J. Basic Appl. Zool.* 2020, 81, 23.
11. Obeng-Gyasi, E. Chronic cadmium exposure and cardiovascular disease in adults. *J. Environ. Sci. Health Part A* 2020, 55, 726–729.
12. Vosahlikova, M.; Roubalova, L.; Cechova, K.; Kaufman, J.; Musil, S.; Miksik, I.; Alda, M.; Svoboda, P. Na<sup>+</sup>/K<sup>+</sup>-ATPase and lipid peroxidation in forebrain cortex and hippocampus of sleep-deprived rats treated with therapeutic lithium concentration for different periods of time. *Prog. Neuro Psychopharmacol. Biol. Psychiatry* 2020, 102, 109953.
13. Hosseinzadeh, Z.; Hauser, S.; Singh, Y.; Pelzl, L.; Schuster, S.; Sharma, Y.; Höflinger, P.; Zacharopoulou, N.; Stournaras, C.; Rathbun, D.L.; et al. Decreased Na<sup>+</sup>/K<sup>+</sup> ATPase expression and depolarized cell membrane in neurons differentiated from chorea-acanthocytosis patients. *Sci. Rep.* 2020, 10, 8391.
14. Gómez-Arnaiz, S.; Tate, R.J.; Grant, M.H. Cytotoxicity of cobalt chloride in brain cell lines—A comparison between astrocytoma and neuroblastoma cells. *Toxicol. Vitro* 2020, 68, 104958.
15. Bejarbaneh, M.; Moradi-Shoeili, Z.; Jalali, A.; Salehzadeh, A. Synthesis of cobalt hydroxide nano-flakes functionalized with glutamic acid and conjugated with thiosemicarbazide for anticancer activities against human breast cancer cells. *Biol. Trace Elem. Res.* 2020, 198, 98–108.
16. Treviño, S.; Díaz, A.; Sánchez-Lara, E.; Sanchez-Gaytan, B.L.; Perez-Aguilar, J.M.; González-Vergara, E. Vanadium in biological action: Chemical, pharmacological aspects, and metabolic implications in diabetes mellitus. *Biol. Trace Elem. Res.* 2019, 188, 68–98.
17. Sánchez-Lara, E.; Treviño, S.; Sánchez-Gaytán, B.L.; Sánchez-Mora, E.; Castro, M.E.; Meléndez-Bustamante, F.J.; Méndez-Rojas, M.A.; González-Vergara, E. Decavanadate salts of cytosine and metformin: A combined experimental-theoretical study of potential metallodrugs against diabetes and cancer. *Front. Chem.* 2018, 6, 402.
18. Zhang, Q.K.; Yue, C.P.; Zhang, Y.; Lu, Y.; Hao, Y.P.; Miao, Y.L.; Li, J.P.; Liu, Z.Y. Six metal-organic frameworks assembled from asymmetric triazole carboxylate ligands: Synthesis, crystal structures, photoluminescence properties and antibacterial activities. *Inorg. Chim. Acta* 2018, 473, 112–120.
19. Wang, X.T.; Li, R.Y.; Liu, A.G.; Yue, C.P.; Wang, S.M.; Cheng, J.J.; Li, J.P.; Liu, Z.Y. Syntheses, crystal structures, antibacterial activities of Cu (II) and Ni (II) complexes based on terpyridine polycarboxylic acid ligand. *J. Mol. Struct.* 2019, 1184, 503–511.
20. Leonardi, G.C.; Falzone, L.; Salemi, R.; Zanghì, A.; Spandidos, D.A.; McCubrey, J.A.; Candido, S.; Libra, M. Cutaneous melanoma: From pathogenesis to therapy. *Int. J. Oncol.* 2018, 52, 1071–1080.
21. Rastrelli, M.; Tropea, S.; Rossi, C.R.; Alaibac, M. Melanoma: Epidemiology, risk factors, pathogenesis, diagnosis and classification. *Vivo* 2014, 28, 1005–1011, PMID: 25398793.
22. Luke, J.J.; Flaherty, K.T.; Ribas, A.; Long, G.V. Targeted agents and immunotherapies: Optimizing outcomes in melanoma. *Nat. Rev. Clin. Oncol.* 2017, 14, 463–482.

23. Paluncic, J.; Kovacevic, Z.; Jansson, P.J.; Kalinowski, D.; Merlot, A.M.; Huang, M.L.-H.; Sahni, S.; Lane, D.J.R.; Richardson, D.R. Roads to melanoma: Key pathways and emerging players in melanoma progression and oncogenic signaling. *Biochim. Biophys. Acta* 2016, 1863, 770–784.
24. Grayschopfer, V.; Wellbrock, C.; Marais, R. Melanoma biology and new targeted therapy. *Nature* 2007, 445, 851–857.
25. Ali, Z.; Yousaf, N.; Larkin, J. Melanoma epidemiology, biology and prognosis. *Eur. J. Cancer Suppl.* 2013, 11, 81–91.
26. Srinivasan, A.; Toh, Y. Human pluripotent stem cell-derived neural crest cells for tissue regeneration and disease modeling. *Front. Mol. Neurosci.* 2019, 12, 39.
27. Mcausland, T.M.; Vloten, J.P.V.; Santry, L.A.; Guilleman, M.M.; Rghei, A.D.; Ferreira, E.M.; Ingraio, J.C.; Arulanandam, R.; Major, P.P.; Susta, L.; et al. Combining vanadyl sulfate with Newcastle disease virus potentiates rapid innate immune-mediated regression with curative potential in murine cancer models. *Mol. Ther. Oncolytics* 2021, 20, 306–324.
28. Jastrzębska, A.M.; Scheibe, B.; Szuplewska, A.; Rozmysłowska-Wojciechowska, A.; Chudy, M.; Aparicio, C.; Scheibe, M.; Janica, I.; Ciesielski, A.; Otyepka, M.; et al. On the rapid in situ oxidation of two-dimensional V<sub>2</sub>CT z MXene in culture cell media and their cytotoxicity. *Mater Sci. Eng. C* 2021, 119, 111431.
29. Das, S.; Roy, A.; Barui, A.K.; Alabbasi, M.M.A.; Kuncha, M.; Sistla, R.; Sreedhar, B.; Patra, C.R. Anti-angiogenic vanadium pentoxide nanoparticles for the treatment of melanoma and their in vivo toxicity study. *Nanoscale* 2020, 12, 7604–7621.
30. Pisano, M.; Arru, C.; Serra, M.; Galleri, G.; Sanna, D.; Garribba, E.; Palmieri, G.; Rozzo, C. Antiproliferative activity of vanadium compounds: Effects on the major malignant melanoma molecular pathways. *Metallomics* 2019, 11, 1687–1699.
31. Rozzo, C.; Sanna, D.; Garribba, E.; Serra, M.; Cantara, A.; Palmieri, G.; Pisano, M. Antitumoral effect of vanadium compounds in malignant melanoma cell lines. *J. Inorg. Biochem.* 2017, 174, 14–24.
32. Farias, C.L.A.; Martinez, G.R.; Cadena, S.M.S.C.; Mercê, A.L.R.; Petkowicz, C.L.; Noleto, G.R. Cytotoxicity of xyloglucan from *Copaifera langsdorffii* and its complex with oxovanadium (IV/V) on B16F10 cells. *Int. J. Biol. Macromol.* 2018, 121, 1019–1028.
33. Ferreira, N.H.; Furtado, R.A.; Ribeiro, A.B.; Oliveira, P.F.; Ozelin, S.D.; Souza, L.D.R.; Neto, F.R.; Miura, B.A.; Magalhães, G.M.; Nassar, E.J.; et al. Europium (III)—Doped yttrium vanadate nanoparticles reduce the toxicity of cisplatin. *J. Inorg. Biochem.* 2018, 182, 9–17.
34. Holder, A.A.; Taylor, P.; Magnusen, A.R.; Moffett, E.T.; Meyer, K.; Hong, Y.; Ramsdale, S.E.; Gordon, M.; Stubbs, J.; Seymour, L.A.; et al. Preliminary anti-cancer photodynamic therapeutic in vitro studies with mixed-metal binuclear ruthenium (II)–vanadium (IV) complexes. *Dalton Trans.* 2013, 42, 11881–11899.
35. Strianese, M.; Basile, A.; Mazzone, A.; Morello, S.; Turco, M.C.; Pellicchia, C. Therapeutic potential of a pyridoxal-based vanadium (IV) complex showing selective cytotoxicity for cancer vs. healthy cells. *J. Cell. Physiol.* 2013, 228, 2202–2209.
36. Burman, B.; Pesci, G.; Zamarin, D. Newcastle disease virus at the forefront of cancer immunotherapy. *Cancers* 2020, 12, 3552.
37. Lacal, P.M.; Failla, C.M.; Pagani, E.; Odorisio, T.; Schietroma, C.; Falcinelli, S.; Zambruno, G.; D'Atr, S. Human melanoma cells secrete and respond to placenta growth factor and vascular endothelial growth factor. *J. Investig. Dermatol.* 2000, 115, 1000–1007.
38. Ogawara, K.; Abe, S.; Un, K.; Yoshizawa, Y.; Kimura, T.; Higaki, K. Determinants for in vivo antitumor effect of angiogenesis inhibitor SU5416 formulated in PEGylated emulsion. *J. Pharm. Sci.* 2014, 103, 2464–2469.
39. Aldini, G.; Altomare, A.; Baron, G.; Vistoli, G.; Carini, M.; Borsani, L.; Sergio, F. N-Acetylcysteine as an antioxidant and disulphide breaking agent: The reasons why. *Free Radic. Res.* 2018, 52, 751–762.